Tellus (1978), *30*, 272–283

Wind-driven circulations in the southwest Baltic

By T. J. SIMONS,[1] *Canada Centre for Inland Waters, Box 5050, Burlington, Ontario L7R 4A6, Canada*

(Manuscript received June 30; in final form October 25, 1977)

ABSTRACT

Wind-driven circulations in the southwest Baltic are analyzed with reference to the combined effects of topography and stratification. Numerical results from a multi-layer nested model are compared with observations taken during the spring of 1975. It appears that the bathymetry and stratification of the southwest Baltic lead to substantial coupling of topographic and baroclinic effects.

1. Introduction

The circulation of shallow, stratified seas is to a large extent controlled by topography and baroclinicity. These effects are of particular importance for the southwest Baltic with its irregular topography and large density gradients. Intrusion of saline water from the North Sea leads to a permanent stratification upon which seasonal temperature variations are superposed. A shallow ridge separates the southwest basin from the open Baltic and tends to prevent exchanges of bottom water. From a dynamical viewpoint, one of the most interesting aspects of this basin is that large depth variations occur at the level of maximum stratification, thus leading to considerable coupling of topographic and baroclinic effects.

Theoretical studies have clarified the role of topography and stratification in the circulation of oceans and atmosphere. Important tools in this effort were the concept of potential vorticity in the absence of stratification and the separation of barotropic and baroclinic modes in the absence of topography. Recent studies of coastal trapped waves have also considered the combined effects of bottom slope and baroclinicity. Like previous theories on the coupling of surface and internal waves, such studies are based on two-layer models with depth variations restricted to the lower layer, such that the equations can be linearized with respect to layer depths. Numerical models permit a quantitative evaluation of the combined effects of complicated topography and stratification encountered in natural basins. This coupling leads to essentially two results. In the first place, baroclinic motions can be excited by barotropic currents crossing depth contours, in contrast to the separable baroclinic motions originating from internal velocity variations such as Ekman currents. In the second place, vertically integrated density anomalies contribute to the potential vorticity balance in the presence of depth variations.

The present study deals with wind-driven circulations in the southwest Baltic, particularly with regard to the effects mentioned above. Numerical techniques are used to simulate currents and density variations for realistic wind forcing and the results are verified by recourse to the "Baltic 75" measurement program. This program was carried out during the spring of 1975 and concentrated on the area north and east of the island Bornholm in the southwest Baltic. Currents and temperatures were recorded continuously at depths of 15, 25, 35, 55, and 65 m in a total of about 20 locations. Additional data were collected by ship cruises, meteorological observations, and mixing experiments. A summary of this experiment has been presented by Keunecke et al. (1975).

This report starts with a discussion of the numerical model. Next, barotropic and baroclinic circulations are considered in the context of

[1] This work was carried out at the Institut für Meereskunde, Kiel, as part of the Program of Canadian-German Collaboration in Oceanography.

idealized forcing conditions and the effects of topography, stratification, friction and boundary conditions are evaluated. Finally, an attempt is made to reproduce the observed circulation in the early part of May, 1975.

2. Numerical model

Numerical simulation of water levels was pioneered many years ago by Hansen (1956) and such models have since been verified by numerous storm surge predictions. In recent years, considerable advances have also been made in three-dimensional models of seas and oceans by borrowing the techniques of numerical weather prediction (see, e.g. Bryan, 1969; National Academy of Sciences, 1975), but verification of these models has been quite limited because of the formidable cost of any observational program suitable for this purpose. For the Baltic Sea, an early modelling study was carried out by Uusitalo (1960) and a review of subsequent experiments has recently been presented by Svansson (1976).

The present three-dimensional model has a free upper surface, but is otherwise similar to typical oceanographic models. Thus the hydrostatic assumption is used together with the Boussinesq approximation, and free convection is simulated by instantaneous adjustment to neutral stability. Horizontal currents are predicted from the equations of motion, vertical motions and surface elevations are obtained from the continuity equation, and temperature and salinity are predicted as the sum of the contributions of advection, diffusion, and surface fluxes. Internal pressure gradients involve density anomalies, which follow from temperature and salinity distributions. Surface wind stress and bottom friction are related to wind and bottom currents, respectively, by the usual quadratic stress laws, while interface fluxes are proportional to vertical gradients in accordance with the conventional gradient hypothesis.

The vertical structure of the multi-layered model consists of a system of fixed permeable levels rather than moving material interfaces. This procedure appears most convenient for dealing with variable stratification and topography combined with baroclinicity. In the horizontal, the variables are staggered to form a lattice structure (Platzman, 1963). In a horizontal plane, the free surface, the vertical velocity, and the density are located at the center of squares, at the sides of which the velocity components are defined. Along the vertical coordinate, density and currents are defined as layer averages, whereas vertical velocities, stresses, and vertical fluxes are specified at levels separating layers. Nearly all computations were performed on a single lattice such that the two horizontal velocity components are defined at different points. For comparison, some solutions were obtained for a double-lattice grid. In the first case, only the normal component was set equal to zero at the shores, in the second case both velocity components go to zero there. The main disadvantage of a double-lattice model is its tendency to produce grid dispersion, whereas a single-lattice model permits spurious inertial frequencies as a result of spatial averaging of the Coriolis term. For instance, the equations for pure inertial motions on a staggered grid between two parallel walls permit oscillations with frequencies $\sigma_n^2 = 0.5f^2\ [1 + \cos n\pi/(N + 1)]$, where N is the number of gridpoints across the channel and n ranges from 1 to N. For high resolutions the eigenfrequencies combine to approach the true inertial oscillation but for low resolutions the error is substantial.

Central differences in time are employed for pressure-divergence terms and forward differences for friction-diffusion terms and all time-extrapolations are carried out by explicit methods. Since the free gravity wave imposes a very small computational time step, the external and internal modes of the model are treated separately. Thus the system of layer equations is transformed into one equation for the vertically averaged flow and a set of equations for the current shears between adjacent layers. The time step for the internal motions is taken to be 15 min. Nonlinear advection terms are treated by a two-step method similar to the Lax–Wendroff scheme. It is verified that the numerical method conserves the volume integral of the predicted variable together with the integrated value of its square.

In principle, the solutions were obtained without allowing for advection or horizontal diffusion of momentum. Experiments with diffusion coefficients of the order of 10^6 cm^2/s indicated that their effects were small, even though this value is larger than those derived from observations by Schott et al. (1976). Horizontal and vertical diffusion of mass was neglected in order not to obscure the transport by currents. Vertical eddy viscosity was varied from 50–100 cm^2/s at the surface to zero at the level of maximum density gradients. The wind stress coefficient was taken to be 1.6×10^{-3} and the bottom stress coefficient was set at 2.5×10^{-3}. A further discussion of the model may be found in the paper by Simons (1974).

The Baltic '75 field experiment covers only a small part of the western Baltic and it was visualized from the outset that a nested system of models should be considered. Nested grid systems or telescopic grids, consisting of fine-mesh domains embedded in larger coarse-mesh domains, are well known from the meteorological literature. The simplest approach is to first calculate the solution for the whole domain with the coarse mesh and then to use this solution only to specify the boundary conditions for the fine-mesh area. Suitable boundary conditions for limited-area integration of the general shallow-water equations have been discussed by Elvius and Sundström (1973) and Chen and Miyakoda (1974). A more complete formulation of a nested model allows for a full interaction between the different grids, including feed-back from the small-scale solution into the outer area (see, e.g., Phillips and Shukla, 1973). In the present case, our interest is essentially limited to the fine-mesh solution and hence it is not necessary to employ an interactive nested model.

In this study a high-resolution model of the southwest Baltic is combined with a low-resolution model of the whole Baltic, in such a fashion that the latter supplies the boundary conditions for the former. For a staggered distribution of variables and in the absence of nonlinear accelerations or horizontal diffusion, these conditions consist of the values of the normal component of the velocity in boundary points. In terms of the present model structure, the boundary velocities are needed in the form of vertically integrated transports and vertical shears. The transport components at the open border of the fine mesh are obtained by interpolation from the coarse mesh in such a fashion that the total transport across the border is conserved. In principle, the vertical shears are to be obtained in the same fashion, and hence the coarse-mesh model should be three-dimensional. For practical purposes, however, it appeared worthwhile to simplify the calculations by the following procedure.

First it is noted that the vertical shears in the

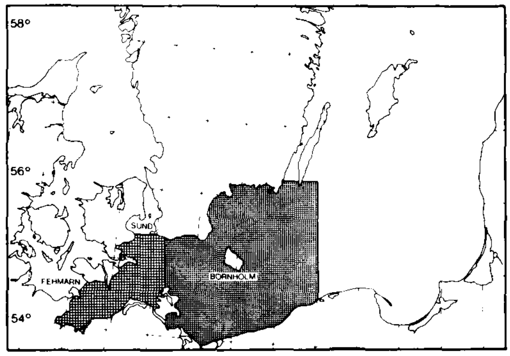

Fig. 1. Location map of Baltic Sea with area of fine-mesh models indicated by shading. Dark shading indicates baroclinic model, light shading represents barotropic fine-mesh model.

boundary points of the fine-mesh model can be predicted immediately if only the baroclinic part of the pressure gradient normal to the border is specified. Furthermore, it will be shown in the following that the stratification during the period of interest is concentrated at a depth of 60 m below the surface. It follows then from the topography of Fig. 2 that the baroclinic response of the area of interest should be essentially independent of the corresponding response of the central Baltic and that the baroclinic part of the pressure gradient along the open border of the fine-mesh model is largely negligible. Thus the assumption is made that this pressure gradient may be approximated by utilizing the density gradients at the first interior row of grid points of the fine mesh. Consequently, the coarse-grid model of the whole Baltic does not need to be baroclinic and is taken to be homogeneous.

The coarse-mesh grid covers the whole Baltic with a mesh size of 20 km. The fine-mesh model covers the southwest Baltic with a mesh size of 5 km. The area of the fine mesh is indicated by shading in Fig. 1. The three-dimensional stratified model is confined to the area shown by dark shading; the light shading indicates a 5-km homogeneous model covering the shallow extreme western part of the Baltic. The stratified model has a vertical resolution of 4 layers concentrated around the level of maximum stratification. Alternatively, the stratified model can have a horizontal grid spacing of 10 km and a vertical resolution of 9 layers with uniform layer depths from top to bottom. The bottom topography for the area covered by the stratified models is shown in Fig. 2.

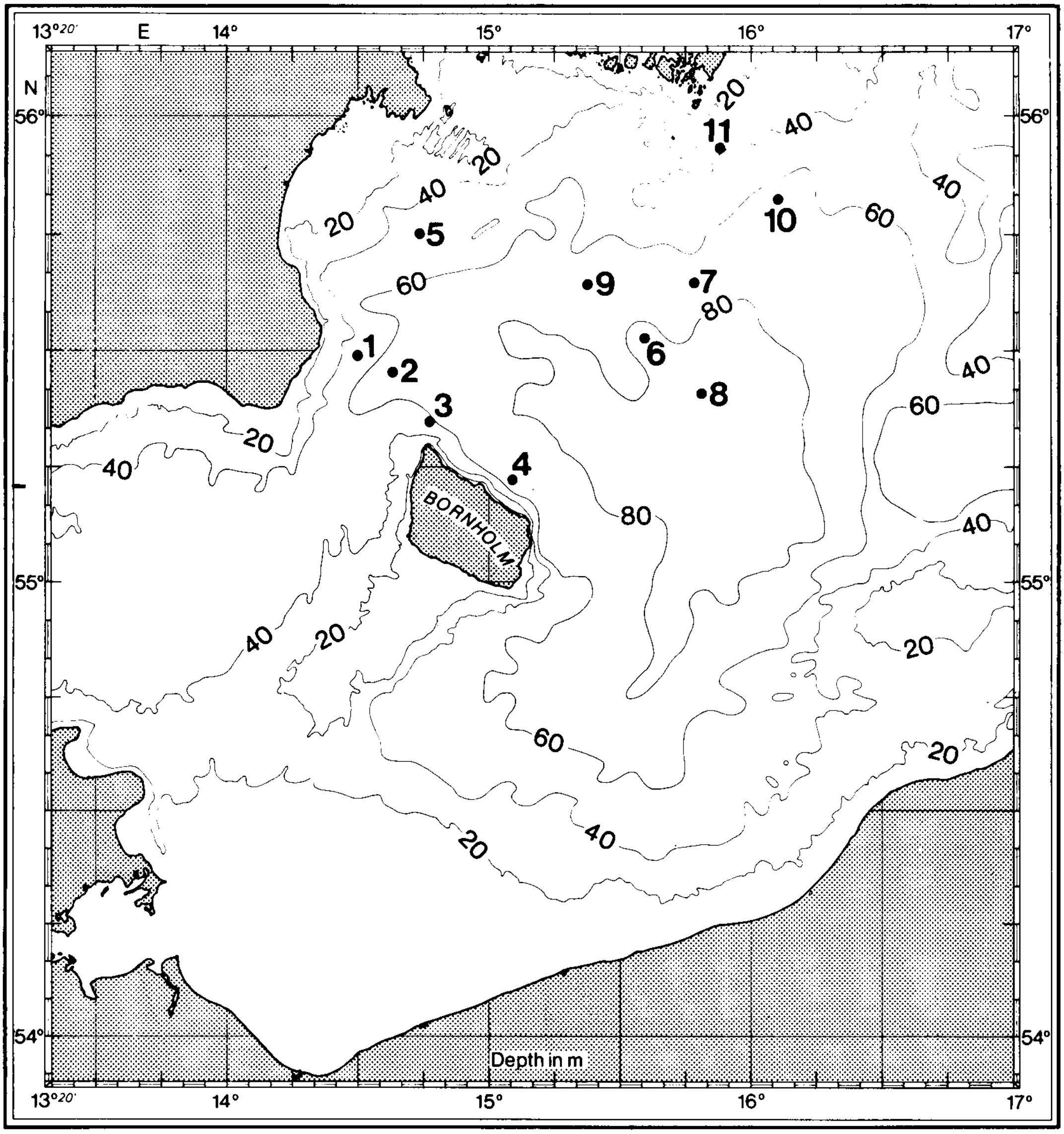

Fig. 2. Topography of SW Baltic (corresponding to dark shading in Fig. 1) and positions of moored instruments during BALTIC 75 field program.

Also shown are the positions of the moored instruments during Baltic '75 which are used for verification.

3. General model solutions

A number of experiments were carried out to investigate the character of water circulations in the southwest Baltic for idealized wind forcing. An analysis was made of effects of friction, boundary conditions, topography, and baroclinicity. With regard to barotropic water motions, the model results were quite consistent with solutions for other similar basins and we will therefore confine ourselves to a very brief summary. On the other hand, the baroclinic calculations indicated an interesting coupling with the bathymetry and they will be discussed in more detail.

The barotropic circulation can be looked upon as a super-position of the vorticity field generated by the interaction of wind and bottom topography, the divergent flow field associated with free surface displacements and the hydraulic flow through the western border of the Baltic. Water motions associated with observed outflow through the Danish Belts (Jacobsen, 1976) were computed to be comparable in magnitude to the directly wind-forced motions for part of the area west of Bornholm Island. The significant effect of this outflow on water levels throughout the Baltic has been amply demonstrated before (see, e.g., Kielmann, 1976). The divergent flow component appears in this study mostly as a periodic water transport across the eastern border of the fine-mesh model. It is associated with the principal surface modes of the whole Baltic which have periods of about a day (Krauss and Magaard, 1962). The corresponding velocities are typically of the order of 1 cm/s. This leaves the topographic flow as the major component of the circulation in the area covered by the Baltic '75 field experiment.

The wind-driven topographic circulation can be best understood by considering the vorticity equation for the vertically averaged flow, which in first approximation may be written.

$$\frac{\partial}{\partial t}(\operatorname{curl} \bar{v}) = \frac{f}{h}\, \bar{v} \cdot \nabla h + \operatorname{curl}\left(\frac{\tau_s - \tau_b}{\rho h}\right)$$

where $\bar{v}$ is the vertical-mean current, t is time, f is the Coriolis parameter, h is the water depth, ∇ is the gradient operator, ρ is density, and τ_s and τ_b represent surface and bottom stress, respectively. In this form, the vorticity balance has been discussed by Groen and Groves (1962) with reference to the fact that wind stress and bottom slope combine to generate vorticity of the mean flow, while the Coriolis effect enters only where the mean flow crosses depth contours. In particular, for a constant wind blowing along depth contours, the forcing term is proportional to $-\tau_s\, \partial h/\partial n$, where n is perpendicular to the isobaths. Hence, if the depth increases (decreases) to the right of the wind, such a wind generates a (counter-) clockwise circulation, i.e., currents in the same direction as the wind in shallow water but in the opposite direction in deep water. This result was noted by Uusitalo (1960) for the Gulf of Bothnia, it was discussed by Rao and Murty (1970) and Bennett (1973) for the Great Lakes, and it will be vividly demonstrated by the subsequent comparison with observations in the Bornholm Basin.

Baroclinic water circulations generally have been studied by recourse to Charney's (1955) formal separation of barotropic and baroclinic modes, thus any vertical displacements of isotherms are related to wind-induced internal velocity distributions rather than vertical-mean flow (see, e.g., Csanady, 1973). In effect, wind-induced interface displacements would be small if the lower layer is shallower than the upper one, as in the western Baltic. However, if the barotropic flow crosses depth contours, the associated divergence of the vertical-mean flow leads to vertical motions which increase towards the bottom, thus presenting a very effective mechanism for generating baroclinic response to wind. Conversely, it is known that bottom topography does not affect the vorticity balance of the vertically integrated transport if pressure gradients due to surface slope and stratification compensate at the bottom (Welander, 1959), but again it has been shown by Holland (1973) that, in practice, topography combined with baroclinicity may lead to considerable enhancement of wind-driven transport. In view of the bathymetry and stratification encountered in the western Baltic, similar effects may be expected to occur here.

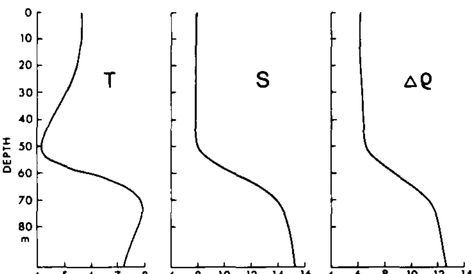

Fig. 3. Vertical profiles of temperature, salinity, and density for Bornholm Basin in early May 1975.

Fig. 3 shows typical vertical profiles of temperature, salinity, and density in the Bornholm Basin for the spring season. These particular profiles were obtained by averaging observations at 27 stations throughout the Basin, during a ship cruise from May 2 to May 5, 1975. Individual profiles showed only minor deviations from this mean. It is seen that the summer thermocline is starting to develop but its effect on the vertical density distribution is still negligible. Homogeneous conditions prevail from the surface down to depths below 50 m, and it is clear that baroclinic effects should be essentially confined to the area within the 60 m depth contour in Fig. 2. It may be recalled that this observation was used previously to justify the purely barotropic boundary conditions at the border between the fine mesh and the coarse mesh.

The density profile of Fig. 3 was adopted as an initial condition for the present three-dimensional model computations. Variations of density were predicted without any horizontal or vertical diffusion to illustrate advection by currents. In the momentum equations vertical eddy viscosity was confined to the upper homogeneous layers of the 9-layer model. In the 4-layer model the upper layer extended down to 50 m and no eddy viscosity was used. Most computations were carried out with the one-lattice 9-layer model as well as with the one-lattice 4-layer model. For comparison a few calculations were done with the double-lattice grid. As expected, the results from the different models were very similar and there is no need to differentiate between them in our discussion. Furthermore, the discussion will be restricted to the solution for a unit-wind stress from the northeast, which approximates the wind episode used for verification in the following section.

The wind-induced variations of the mass field can be best illustrated by concentrating on the model layer between 60 and 70 m. The density field for this layer after 3 days of NE wind is shown in Fig. 4. In order to separate the contributions of the stress-induced vertical velocities from the effects of the topographically induced vertical-mean flow, the computations were repeated with the latter set equal to zero. This result is shown in Fig. 5. The density distribution of Fig. 5 will be recognized immediately as a result of surface Ekman drift to the right of the wind and compensating pressure gradient currents below. This is a typical solution for the case where the barotropic and baroclinic flow components can be separated. On the other hand, Fig. 4 includes the additional effects of barotropic flow crossing depth contours with the associated horizontal divergence of the vertical-mean current. Comparison of Figs. 4 and 5 shows that such coupling effects of topography and baroclinicity are here at least as large as the separable baroclinic solution. As a result, the response to wind becomes difficult to analyze on the basis of the concepts of conventional baroclinic theory and Ekman dynamics.

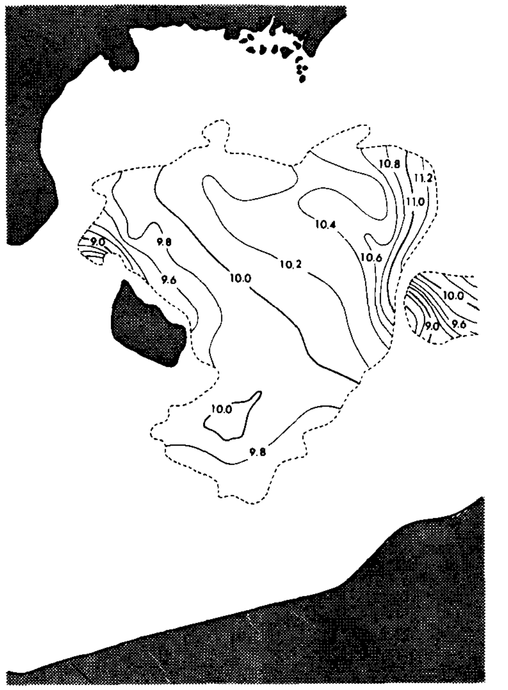

Fig. 4. Density anomaly for model layer between 60 and 70 m after three days of NE wind with realistic outflow through Danish Belts.

In view of the close relationship between vertical variations of the flow field and horizontal gradients of the mass field, the topographic circulation will also affect the internal current distribution. Such effects are particularly noticeable within the shallow layer below the maximum density gradient. Since the computed baroclinic currents are clearly in agreement with the mass field, it would be superfluous to show the results here. Not so straightforward is the reverse effect of stratification on vertical-mean flow in the presence of depth variations. It follows from the complete vorticity equation that there are two possible effects, namely, a change of bottom stress due to baroclinic currents in the deep layers, and the orientation of vertically integrated density anomalies relative to depth contours. In the numerical model such effects can be readily separated by including baroclinicity in the vertical shearing flow without allowing for density effects on the mean flow. In the

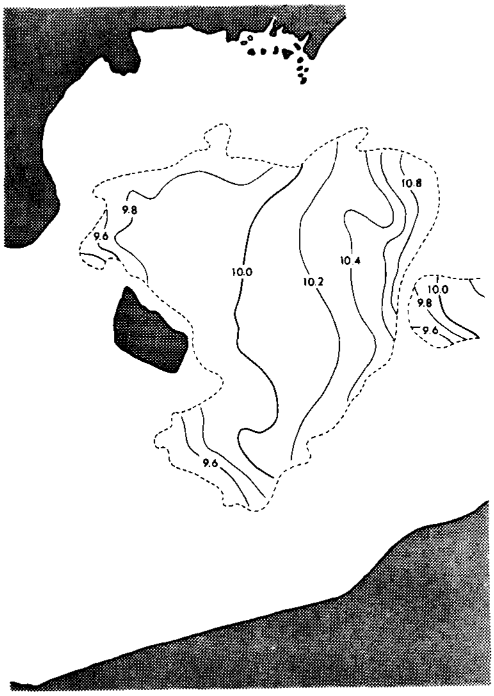

Fig. 5. Same as Fig. 4, but excluding effects of vertical-mean topographic circulation.

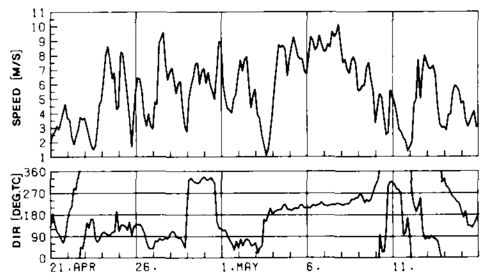

Fig. 6. Wind measured over water at position of mooring 6 during BALTIC 75 (Fig. 2).

latter case, vertically averaged solutions were found to be almost indistinguishable from multi-layer barotropic results. By contrast, substantial changes of vertically integrated transport are found in the stratified part of the basin if density effects are fully included. For a visual inspection of these circulations and others discussed in this section, the reader is referred to Simons (1976).

4. Comparison with observations

Verification of model computations requires detailed knowledge of wind forcing as well as current and density observations. It is likely that the most meaningful results will be obtained if one can isolate a particular wind event whose inpact on water movements overshadows the effects of regular day-to-day meteorological disturbances. Such a wind episode occurred during the first 10 days of May, 1975. Although the wind speed, measured over water, never exceeded 8 m/s, the storm persisted for nearly a whole week with wind direction shifting only slightly from N to NE. Fig. 6 shows the relevant part of the wind record taken near current meter mooring 6 (Fig. 2) during the Baltic '75 field program. The wind event in the early part of May was adopted for the present verification analysis. All model runs were started from rest, beginning 10 days before the onset of the storm, namely, on April 24, 1975. Except for the deep, stratified, part of the basin, this period should be long enough for the bottom friction to damp out effects of erroneous initial conditions. This is confirmed by a comparison of observed and computed currents before the storm, which will be shown in Fig. 7.

The positions of the moored current meters used in this study were shown earlier in Fig. 2. A complete listing of the available current records for this period is presented in Table 1, together with the sounding depths in each station. Station 6 consisted actually of a small-scale array of moorings with horizontal separations of the order of 1 km. For the present purpose, this so-called "inner nest" can be treated as a single station. Individual records within the inner nest and simultaneous drift measurements show reasonably consistent results if proper allowance is made for the different types of instruments used (Schott et al., 1975). The data used here were taken from stations 6A and 6E at the center of the inner nest. Finally, it should be noted that station 5 was actually numbered mooring 15 during the Baltic '75 field program.

As a first approach to model verification it should be established to what extent the observed water transports can be simulated by a conventional homogeneous storm-surge model. Thus the barotropic nested model discussed in Section 4 was run for the period April 24 to May 15, 1975, with outflow through the Danish Belts prescribed on the basis of observations. A quadratic formulation of wind stress was used with a coefficient equal to 1.6 $\times$ 10^{-3}. A linear bottom stress, inversely proportional to the square of the depth with a coefficient of 50 cm^2/s, was incorporated in the first run, approximating Platzman's (1963) solution of the Ekman equations. The results were averaged over 28 hours, eliminating inertial motions with periods of about 14 hours, as well as the major contributions of the free surface modes with periods a little over 1 day. Figs. 7 and 8 show synoptic distributions of vertical-mean currents before and after the storm of May 3–9, 1975. A vector length equal to the grid mesh represents a velocity of 20 cm/s. Although the fine-mesh model covered the whole southwest Baltic, results are shown only for the Baltic '75 measurement area.

For comparison with these model results, a scheme must be adopted to estimate vertically integrated water transports from observed currents at 15, 25, 35, 55, and 65 m. In this case it was decided to use the simplest possible averaging procedure consistent with the stratification of Fig. 3. Thus a two-layer structure was postulated with an interface depth of 50 m and the flow in the upper (lower) layer equal to the arithmetic mean of all observations above (below) the interface. Again the results were averaged over 28 hours and then entered at the proper locations in Figs. 7 and 8.

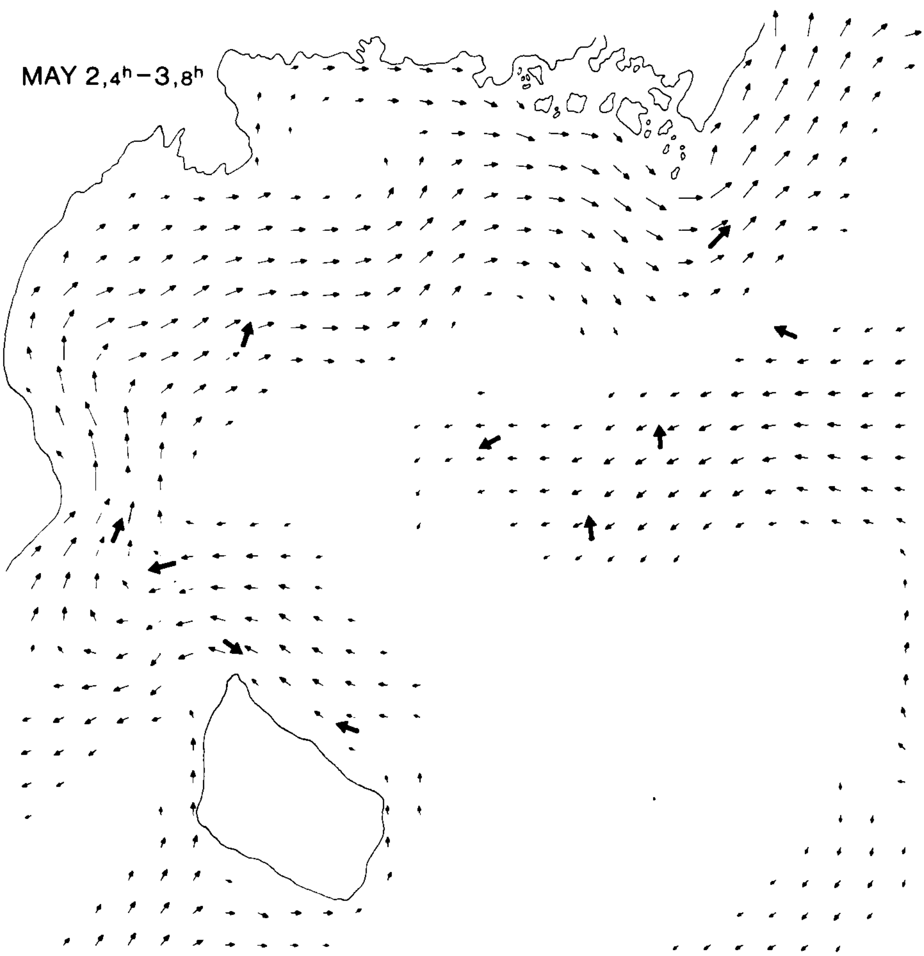

Fig. 7. Vertical-mean currents computed with a barotropic model (light arrows), together with corresponding currents estimated from observations (dark arrows), before the storm of May 3, 1975.

Table 1. *Moored current meters during period May 1-15, 1975*

Position	Water depth	Instrument depths (in meters)				
1	48	15		35		
2	78	15	25	35	55	65
3	69	16	26	36		65
4	64	15	25	35	55	61
5	55	15		35		
6	74	approx. 25 current meters in 7 moorings				
7	69		25	35	55	64
8	90					
9	70	15		35	55	65
10	61		25	35	55	
11	38		25	35		

Figs. 7 and 8 indicate immediately that the observations confirm the basic concept of large-scale vorticity being generated by the interaction of wind stress and bottom slope as discussed in the previous section. Thus the clockwise circulation dominating before the storm (Fig. 7) is completely reversed by the end of this wind event (Fig. 8). In particular, at that time the agreement between model and observations is remarkably good. Some interesting discrepancies appear at intermediate times, suggesting that the flow reversal in nature occurs slower than in the model. Furthermore, as expected, the correspondence between model results and measurement deteriorates somewhat after the storm, when the flow breaks up in a number of counter-rotating cells moving around the basin. Such circulation cells are typically found

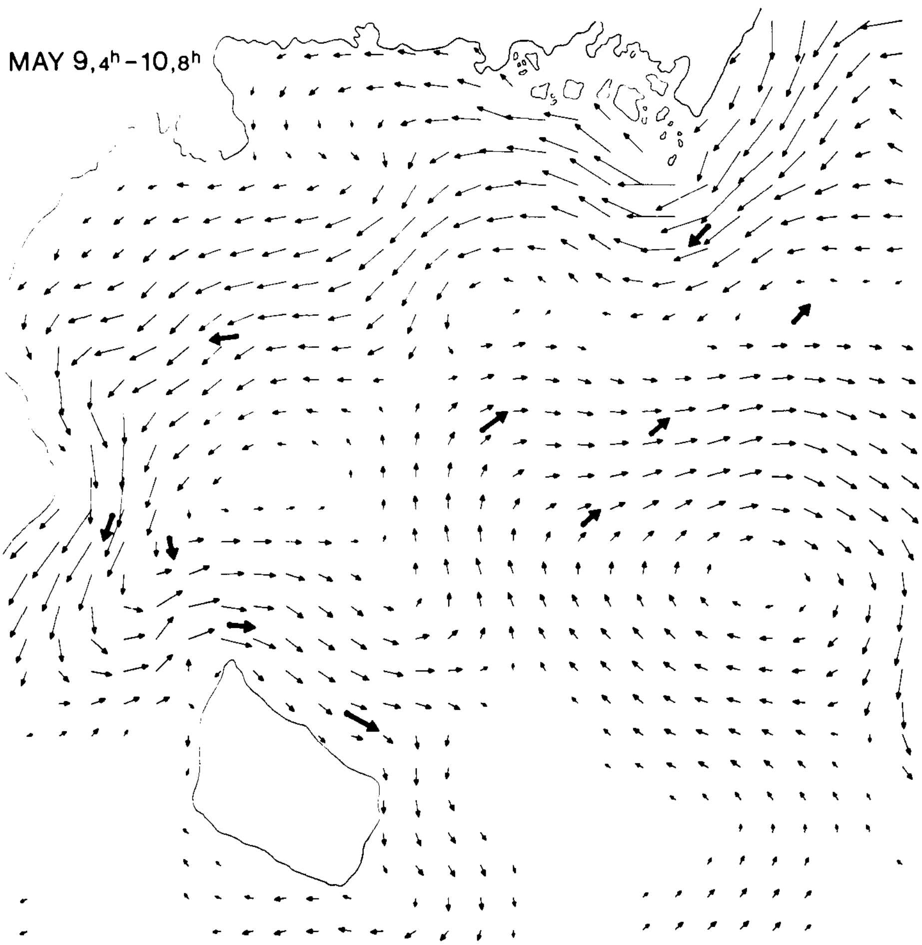

Fig. 8. Vertical-mean currents computed with a barotropic model (light arrows), together with corresponding currents estimated from observations (dark arrows), after the storm of May 3, 1975.

in the so-called topographic modes of oscillation of a basin with irregular bottom topography.

For a more detailed analysis and verification it is convenient to consider time series of observed and computed currents as a function of depth for given locations. Here results will be presented from the 9-layer baroclinic model with uniform layer depths of 10 m. The model was started from rest on April 24, 1975, with the density distribution shown in Fig. 3. Computed currents were simply taken from model grid points closest to the corresponding observation stations. Again the currents are averaged over 28 hours for this comparison.

The upper part of Fig. 9 shows results for station 1 along the northern shore of the Bornholm Channel. Here the water depth is only 48 m and the vertical variation of currents with depth is essentially due to frictional effects only. Apparently, this vertical shear is well simulated by the model, thus indicating that eddy viscosity effects are properly taken into account. However, during the first half of the storm, the observations suggest a vertical-mean flow in a northerly direction (against the wind), whereas the model computes a southward transport. Recalling that the model computes vertical-mean flow and vertical shears separately, it appears clear that possible improvement of this result can be achieved only by a better simulation of the barotropic flow component, i.e. the balance between surface pressure gradient and wind and bottom stresses.

The lower part of Fig. 9 presents results for station 2 in the middle of the Bornholm Channel. To facilitate a visual comparison of observations and model results, currents are shown only for 15, 35, and 65 m. A two-layer structure is clearly indicated, with only minor vertical shears within the upper layer. The vertical shears between 35 and 65 m are almost completely due to baroclinic effects. This was verified by running the same model without stratification. Thus these observations tend to support the baroclinic computations discussed in the previous section. In this case, the vertically integrated transport also appears quite well reproduced by the model, thus confirming that the transport in deep water tends to run against the wind.

More complicated appears the observed water circulation along the shore of Bornholm Island, in particular in station 4. This is shown in the upper

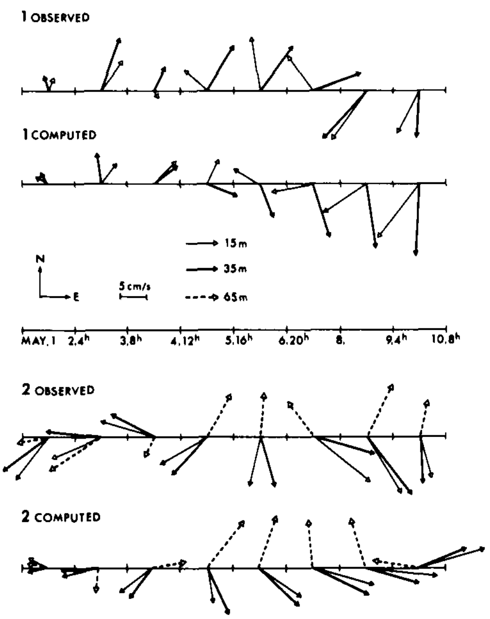

Fig. 9. Observed and computed currents, averaged over 28 hours, for station 1 (above) and station 2 (below) in the Bornholm Channel.

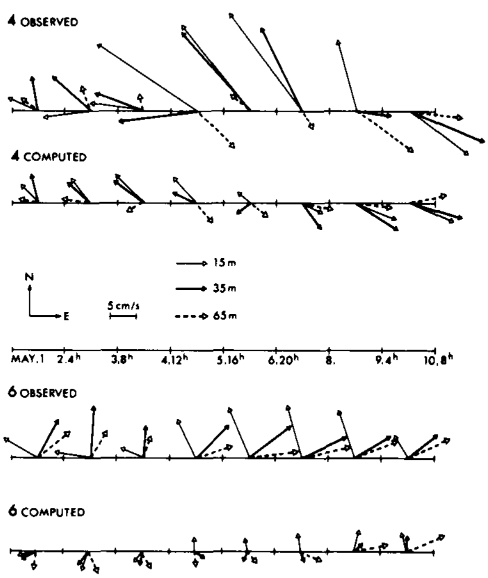

Fig. 10. Same as Fig. 9, but for nearshore station 4 (above) and offshore station 6 (below).

part of Fig. 10. Again, at the beginning of the storm, May 4–5, there is a tendency for the model to properly reproduce the baroclinic shears between the upper and lower layers, although the observed shearing motions are substantially larger in magnitude. Most surprising, however, is the sudden increase of current velocities throughout the upper homogeneous layer. Since the local water depth is only 64 m, it appears likely that there is a large net water transport in the northerly direction along the shore. This could tie in with the northerly flow at station 1 for the same period, May 5–8. It may be noted that this longshore transport is at right angles to the wind and, consequently, the direct effect of the wind stress on this component of the vertically integrated flow should be negligible. This would point to the surface pressure as the source of the observed accelerations. At any rate, the phenomenon disappears as suddenly as it appeared and the subsequent currents are remarkably similar in the model and in nature.

The remaining shallow water stations, 5, 10, and 11, behave typically like station 1 (see also Figs. 7–8). In all these stations the agreement between model and observations appears acceptable. The deep water stations (6, 7, 9) show a quite different pattern. As an example, station 6 is shown in the lower part of Fig. 10. In this case, as for all offshore stations, the prevailing direction of the water transport is against the wind, but the magnitude of the observed currents is consistently underestimated by the model. The difference can be largely traced to erroneous initial conditions. Even though the model was started 10 days before the storm, the computed deep water circulation at the onset of the storm appears much weaker than the observed water movements. It should be noted, however, that there are indications that the moored current meters overestimated actual current speeds. Thus, drift measurements by Schott et al. (1975) for this storm period and this area show mean speeds of about 5 cm/s and directions varying from N to NE between the surface and 30 m. The observed currents in station 6 are about twice as large, the computed ones about half as large as the drifters indicate.

All in all it is evident that it would be a difficult task to properly model the circulation of the deep basin. As demonstrated by the numerical results, the circulation consists of closed cells which migrate continually through the basin. The currents at any given point depend on its position relative to these cells and small errors in position will lead to completely different currents in a model gridpoint which is used for verification. It is known that water movements in this deep, stratified basin can persist for very long periods so that observed circulations cannot be related to known forcing functions in a straight-forward manner. This leads to a build-up of momentum and is probably the reason for the discrepancies between the model and observations with regard to current speeds in deep water.

On the other hand it is gratifying to see that present modeling techniques are capable of simulating many of the more striking aspects of observed water motions and, in doing so, confirm the results and conclusions of earlier conceptual models of large-scale circulation in the sea.

5. Acknowledgements

This research was supported by the Fraunhofer-Gesellschaft, München, and by the Program of Canadian-German Collaboration in Oceanography. Computer time was made available by the University Computing Centre, Kiel.

The author gratefully acknowledges the valuable help and advice from the staff of the Institut für Meereskunde, in particular, Prof. W. Krauss, Mr J. Kielmann, Mr J. Holtorff, and Ms D. Raasch.

REFERENCES

Bennett, J. R. 1974. On the dynamics of wind-driven lake currents. *J. Phys. Oceanogr. 4*, 400–414.

Bryan, K. 1969. A numerical method for the study of ocean circulation. *J. Comput. Phys. 4*, 347–376.

Charney, J. G. 1955. Generation of oceanic currents by wind. *J. Mar. Res. 14*, 477–498.

Chen, J. H. and Miyakoda, K. 1974. A nested grid computation for the barotropic surface atmosphere. *Mon. Wea. Rev. 102*, 181–190.

Csanady, G. T. 1973. Transverse internal seiches in large oblong lakes and marginal seas. *J. Phys. Oceanogr. 3*, 439–447.

Elvius, T. and Sundström, A. 1973. Computationally efficient schemes and boundary conditions for a fine-mesh barotropic model based on the shallow water equation. *Tellus 25*, 132–156.

Groen, P. and Groves, G. W. 1962. Surges. *The sea* (ed. M. N. Hill), Vol. 1. New York: Interscience, pp. 611–647.

Hansen, W. 1956. Theorie zur Errechnung des Wasserstandes und der Strömungen in Randmeeren nebst Anwendungen. *Tellus 8*, 287–300.

Holland, W R. 1973. Baroclinic and topographic influences on the transport in western boundary currents. *Geophys. Fluid Dyn. 4*, 187–210.

Jacobsen, T. 1976. Preliminary transport calculations in the Great Belt. Proc. 10th Conf. Baltic Oceanogr., Göteborg, June 2–4, 1976.

Keunecke, K. H., Kohn, H., Krauss, W., Miosga, G., Schott, F., Speth, P., Willebrand, J. and Zenk, W. 1975. *Baltic 75, Physikalischer Teil.* Institut für Meereskunde, Universität Kiel, Bericht Nr 11.

Kielmann, J. 1976. Numerical modelling in connection with Baltic 75. Proc. 10th Conf. Baltic Oceanogr., Göteborg, June 2–4, 1976.

Krauss, W. and Magaard, L. 1962. Zum System der Eigenschwingungen der Ostsee. *Kieler Meeresforschungen 18*, 184–186.

National Academy of Sciences. 1975. *Numerical models of ocean circulation.* Proc. Symp. Durham, N. H., October 17–20, 1972.

Phillips, N. A. and Shukla, J. 1973. On the strategy of combining coarse and fine grid meshes in numerical weather prediction. *J. Appl. Meteor. 12*, 763–770.

Platzman, G. W. 1963. The dynamical prediction of wind tides on Lake Erie. *Meteor. Monogr. 4*, No. 26.

Rao, D. B. and Murty, T. S. 1970. Calculations of the steady state wind-driven circulation in Lake Ontario. *Arch. Meteor. Geophys. Bioklim.* A *19*, 195–210.

Schott, F., Ehlers, M., Hubrich, L. M. and Quadfasel, D. 1976. *On measurements of horizontal mass and momentum transfer in small scales during BALTIC 75.* Institut für Meereskunde, Universität Kiel.

Simons, T. J. 1974. Verification of numerical models of Lake Ontario. Part 1: Circulation in spring and early summer. *J. Phys. Oceanogr. 4*, 507–523.

Simons, T. J. 1976. *Topographic and baroclinic circulations in the southwest Baltic.* Institut für Meereskunde, Universität Kiel, Bericht Nr 25.

Svansson, A. 1976. The Baltic circulation: A review in relation to ICES/SCOR Task 3. Proc. 10th Conf. Baltic Oceanogr., Göteborg, June 2–4, 1976.

Uusitalo, S. 1960. The numerical calculation of wind effect on sea level elevations. *Tellus 12*, 427–435.

Welander, P. 1959. On the vertically integrated mass transport in the oceans. In *The atmosphere and the sea in motion* (ed. B. Bolin). New York: The Rockefeller Institute Press, pp. 95–101.

ВЕТРОВЫЕ ЦИРКУЛЯЦИИ В ЮГО- ЗАПАДНОЙ ЧАСТИ БАЛТИЙСКОГО МОРЯ

С учетом комбинированных эффектов топографии и стратификации анализируются вызванные ветром циркуляции в юго-западной части Балтийского моря. Численные результаты, полученные с помощью многоуровенной модели с учащенной сеткой, сравниваются с данными наблюдений, проведенных весной 1975 г. Представляется, что рельеф дна и статификация в юго-западной Балтике вызывают существенное взаимодействие топографических и бароклинных эффектов.